Electronic Supplementary Material (ESI) for Physical Chemistry Chemical Physics.
This journal is © the Owner Societies 2018

ELECTRONIC SUPPLEMENTARY INFORMATION (ESI)

Anionic Merocyanine Dyes Based on Thiazol-2-Hydrazides: Reverse Solvatochromism, Preferential Solvation and Multiparametric Approaches to Spectral Shifts

Arindam Mukhopadhyay,* Krishna J. Mandal and Jarugu Narasimha Moorthy*
Department of Chemistry, Indian Institute of Technology, Kanpur 208016, INDIA
* Corresponding authors,
E-mail: arindam389@gmail.com (for AM) and moorthy@iitk.ac.in (for JNM)

CONTENTS

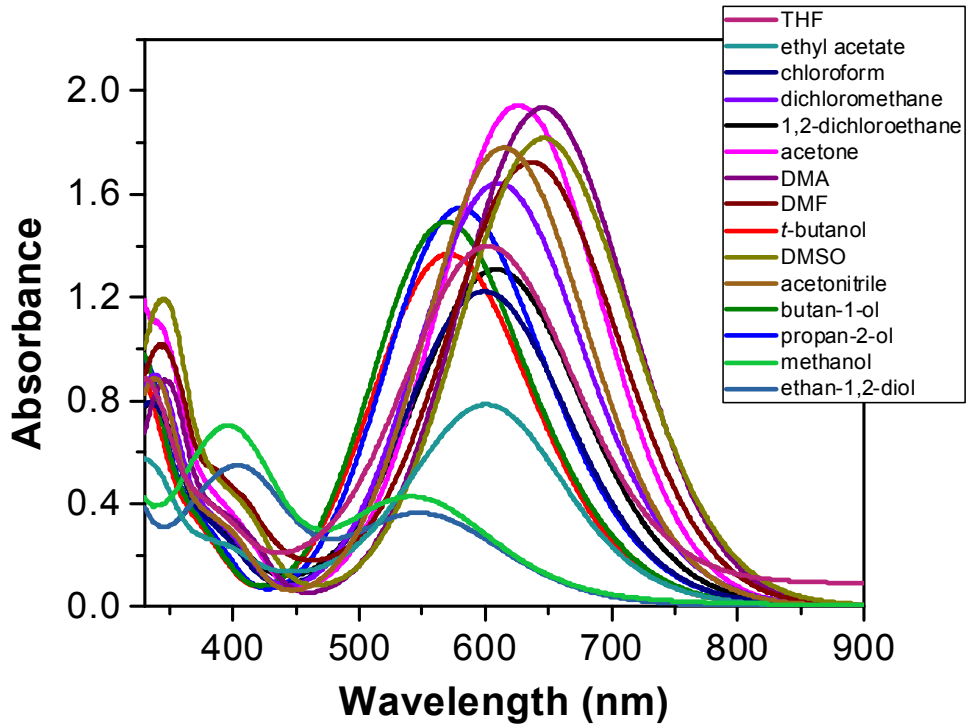

Figure S1. UV-vis absorption spectra of **THA1** (50 μM) in different solvents.

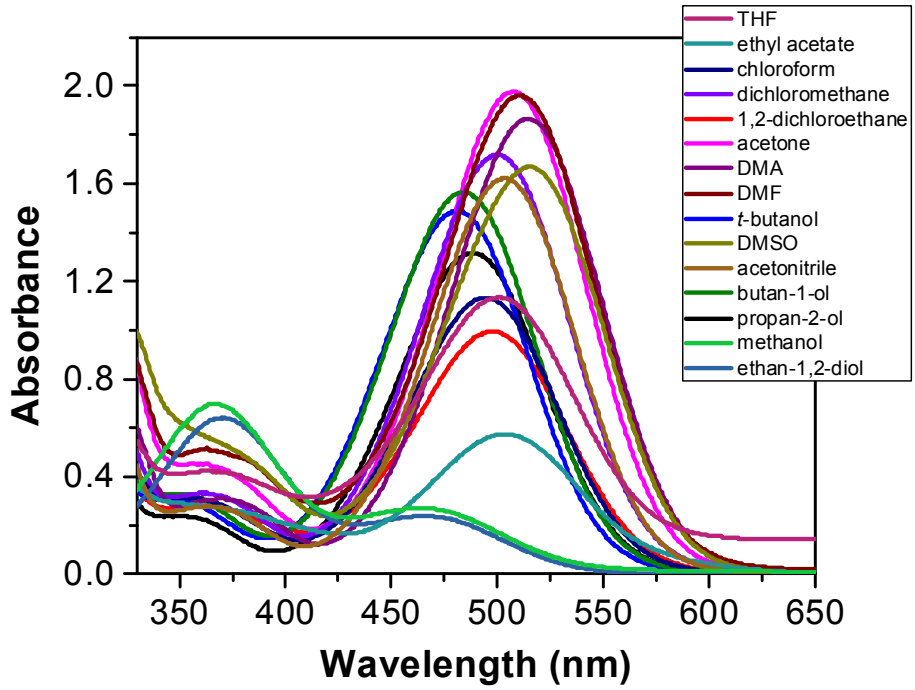

Figure S2. UV-vis absorption spectra of **THA2** (50 μM) in different solvents.

Spectrophotometric Experiments to Reveal the Influence of Counter Cation. To investigate whether or not the anionic **THA** dyes form ion pair with the counter cation, UV-vis absorption spectra of the **THA**s (50 μM) were recorded in the presence of excess of tetra-*n*-butylammonium iodide, i.e., TBAI (concentration = 1 mM, i.e., 20 equivalents) in THF as a representative solvent. As shown below, the absorption maximum of both **THA1** (603 nm) and **THA2** (501 nm) was found to remain the same before and after the addition of TBAI. This experiment, thus, establishes the fact that the TBA cation doesn't form ion pair with the anionic **THA** dyes. Similar results were also obtained by Machado and co-workers.[1]

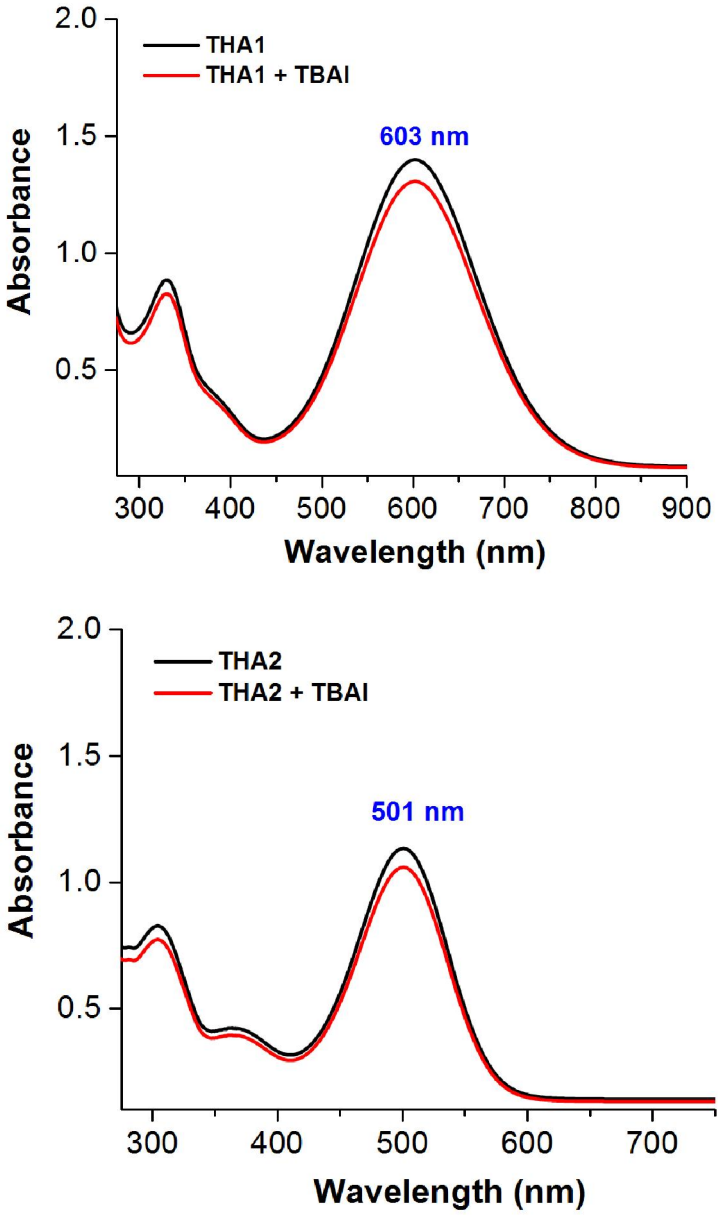

Figure S3. UV-vis absorption spectra (50 μM) of **THA1** (top) and **THA2** (bottom) in the absence (black line) and in the presence (red line) of TBAI (1 mM) in THF.

To further investigate the influence of other counter cation, such as K^+, the deprotonation of **TH1**, a representative case, in THF (50 μM) was carried out in the presence of aq. KOH (5×10^{-4} M, i.e., 10 equivalents). The λ_{max} of the colored solution (**THA1**) in this case was found to be at 558 nm, which is 45 nm blue shifted when compared to that of the colored solution generated in the presence of TBAOH (λ_{max} = 603 nm). This suggests strong electrostatic interaction between the hydrazide anion and K^+ cation. However, when this colored solution was treated with excess (5×10^{-3} M) of 18-crown-6, a highly selective receptor of K^+, the absorption spectrum was found to be almost the same which is obtained in the presence of TBAOH (5×10^{-4} M) in THF. This compellingly attests to the fact that the TBA cation doesn't have any influence on the spectral properties of the anionic dyes. Similar results were also obtained by Machado and co-workers.[1]

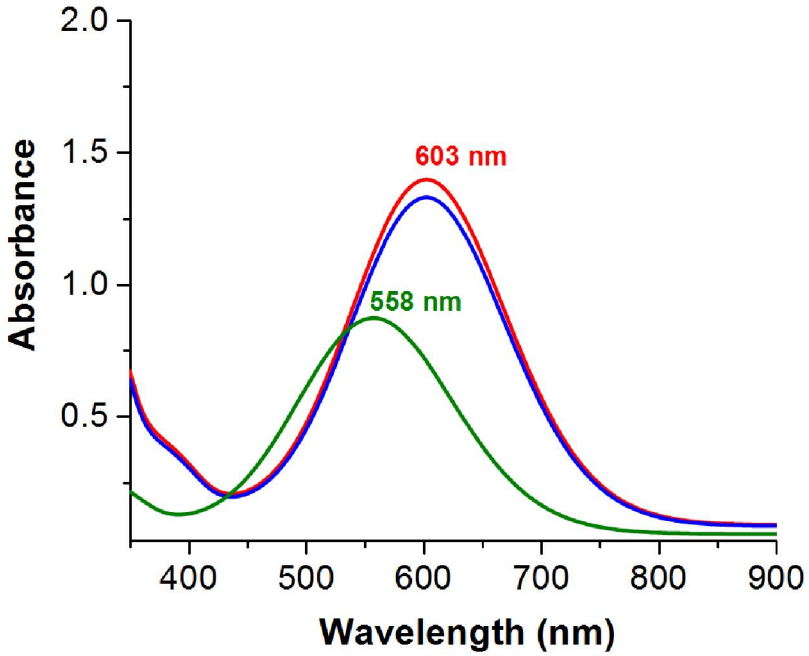

Figure S4. UV-vis absorption spectra of **THA1** in THF under different conditions.
Red line: When the deprotonation of **TH1** (50 μM) is carried out using TBAOH (5×10^{-4} M);
Green line: When the deprotonation of **TH1** (50 μM) is carried out using KOH (5×10^{-4} M);
and Blue line: After addition of excess of 18-crown-6 (5×10^{-3} M) to the solution of **THA1** deprotonated with KOH. Notice that the absorption maxima of the red and blue lines are the same.

Spectrophotometric Experiments Employed to Discard the Possibility of Auto-Aggregation of THAs. To establish the fact that auto-aggregation of the **THA** dyes doesn't take place at the concentration (50 μM) used for solvatochromic studies, we followed the methodology established by El Seoud and co-workers.[2] Accordingly, the absorbances of the solutions of the **THA**s were plotted with increasing concentration of the latter in the range of ca. 5×10^{-6} M to 7×10^{-5} M in three representative solvents, namely, THF, MeCN and MeOH. As shown below, all the plots of absorbance versus concentration were found to be linear with excellent goodness-of-fit ($R^2 = 0.99$) values. This means that Beer's law holds true for them and therefore, this establishes that self-aggregation of the **THA** dyes doesn't occur in this concentration range.

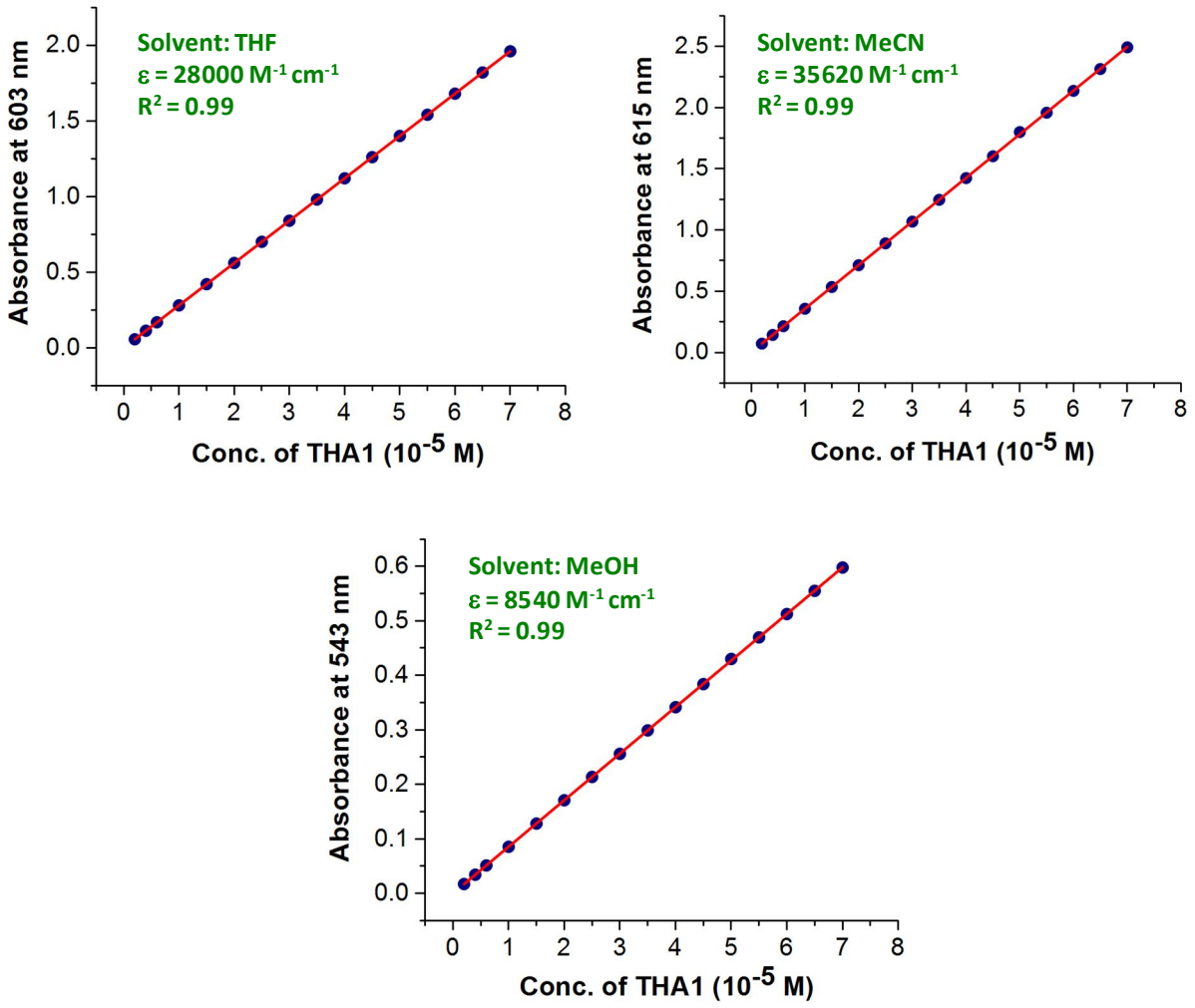

Figure S5. Linear plot of the absorbance (at the λ_{max}) versus concentration of **THA1** in different solvents.

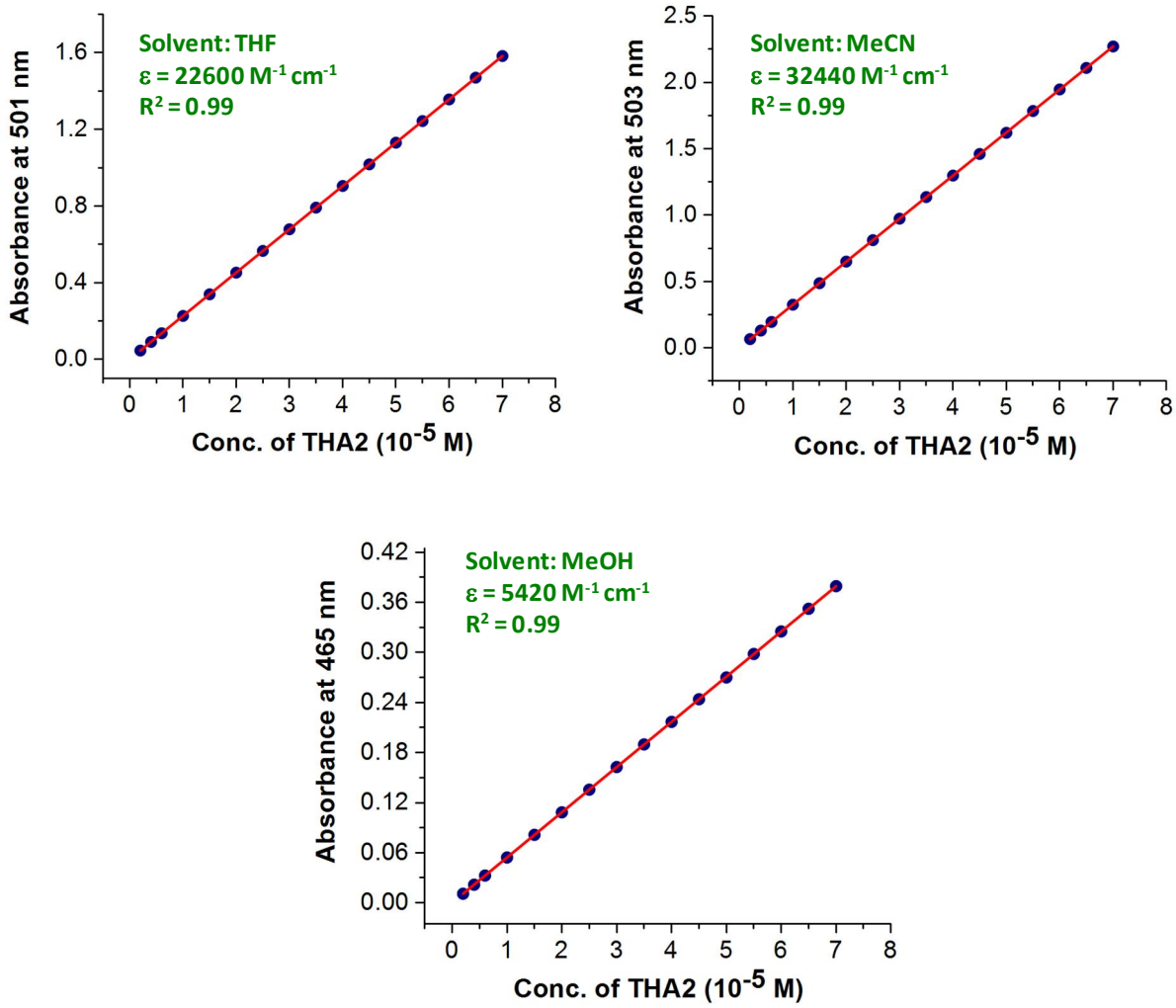

Figure S6. Linear plot of the absorbance (at the λ_{max}) versus concentration of **THA2** in different solvents.

Changes in ^{1}H NMR Signals of TH2 upon Addition of TBAOH. The changes in the ^{1}H NMR signals of **TH2** upon addition of TBAOH are shown below. Accordingly one observes the following: i) the doublets (H_f and H_g) corresponding to 4-cyanophenyl ring undergo substantial upfield shifts (ca. 0.23-0.26 ppm); ii) while the singlet corresponding to the benzylidene proton (H_e) undergoes an upfield shift of ca. 0.20 ppm, the singlet proton of the thiazole ring (H_a) undergoes highest upfield shift of ca. 0.50 ppm; and iii) the protons of the phenyl ring (H_b, H_c and H_d) substituted at position 4 of the thiazole ring undergo only marginal upfield shifts.

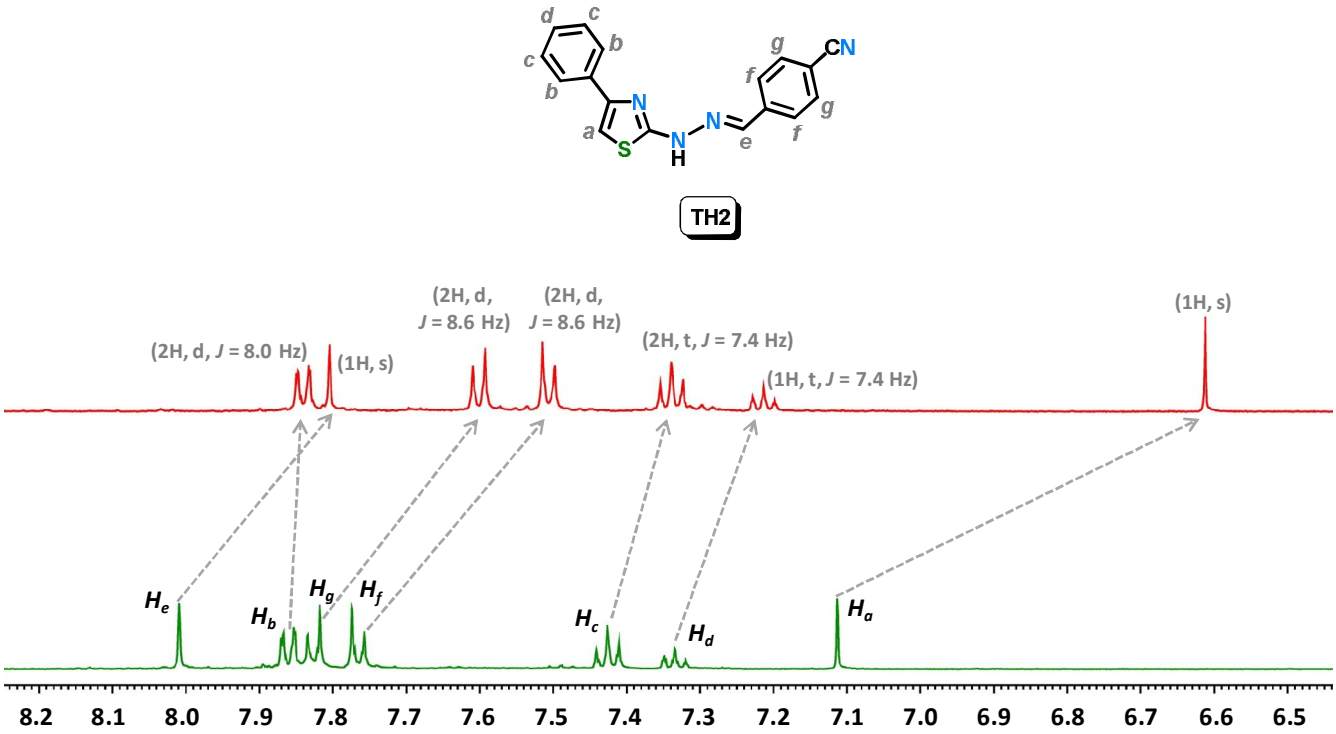

Figure S7. ^{1}H NMR (500 MHz) spectra of **TH2** (0.03 M) in CD_3CN before (green) and after (red) addition of excess (ca. 10 molar equivalents) TBAOH.

Table S1. Preferential solvation study of **THA1** in a binary solvent mixture.

Binary mixture of solvents	X_2	X_2^L	$X_1^L = (1 - X_2^L)$	λ_{max} (nm)	$\bar{\upsilon}_{12}$ (cm^{-1})	$\delta_{s2} = (X_2^L - X_2)$	K_{12}
acetonitrile (X_1) and methanol (X_2)	0.0285	0.18854	0.81146	600	16666.67	0.16004	0.12628
	0.05543	0.293	0.707	592	16891.89	0.23758	0.14159
	0.10504	0.41395	0.58605	583	17152.66	0.30892	0.16616
	0.14969	0.49668	0.50332	577	17331.02	0.34699	0.1784
	0.22685	0.58114	0.41886	571	17513.13	0.3543	0.21147
	0.29117	0.6529	0.3471	566	17667.84	0.36173	0.21838
	0.34561	0.69657	0.30343	563	17761.99	0.35096	0.23006
	0.39228	0.7407	0.2593	560	17857.14	0.34842	0.22597
	0.43274	0.77039	0.22961	558	17921.15	0.33765	0.22737
	0.46815	0.80028	0.19972	556	17985.61	0.33214	0.21966
	0.4994	0.81532	0.18468	555	18018.018	0.31592	0.22597
	0.52717	0.8304	0.1696	554	18050.54	0.30323	0.22772
	0.55203	0.84554	0.15446	553	18083.18	0.29351	0.22511
	0.56351	0.84554	0.15446	553	18083.18	0.28203	0.23583
	0.58679	0.86073	0.13927	552	18115.94	0.27394	0.22977
	0.61208	0.87598	0.12402	551	18148.82	0.2639	0.22339
	0.63965	0.89129	0.10871	550	18181.82	0.25163	0.21651
	0.66983	0.90665	0.09335	549	18214.94	0.23682	0.20888
	0.70298	0.92207	0.07793	548	18248.17	0.21908	0.20005
	0.7396	0.93754	0.06246	547	18281.53	0.19794	0.18922
	0.78023	0.93754	0.06246	547	18281.53	0.15731	0.23653
	0.82559	0.95307	0.04693	546	18315.02	0.12748	0.2331
	0.87655	0.9843	0.0157	544	18382.35	0.10775	0.11327
	0.93421	0.9843	0.0157	544	18382.35	0.05008	0.22653

Table S2. Preferential solvation study of **THA2** in a binary solvent mixture.

Binary mixture of solvents	X_2	X_2^L	$X_1^L = (1 - X_2^L)$	λ_{max} (nm)	$\bar{\upsilon}_{12}$ (cm^{-1})	$\delta_{s2} = (X_2^L - X_2)$	K_{12}
acetonitrile (X_1) and methanol (X_2)	0.0285	0.12286	0.87714	498	20080.32	0.09436	0.20945
	0.05543	0.24821	0.75179	493	20283.97	0.19278	0.17774
	0.10504	0.32465	0.67535	490	20408.16	0.21961	0.24415
	0.14969	0.37613	0.62387	488	20491.80	0.22644	0.29199
	0.22685	0.42804	0.57196	486	20576.13	0.20119	0.39207
	0.29117	0.48037	0.51963	484	20661.15	0.1892	0.44435
	0.34561	0.53314	0.46686	482	20746.88	0.18753	0.46248
	0.39228	0.58635	0.41365	480	20833.33	0.19407	0.45538
	0.43274	0.61312	0.38688	479	20876.82	0.18038	0.48137
	0.46815	0.64	0.36	478	20920.50	0.17185	0.49513
	0.4994	0.667	0.333	477	20964.36	0.1676	0.49806
	0.52717	0.6941	0.3059	476	21008.40	0.16693	0.49136
	0.55203	0.72133	0.27867	475	21052.63	0.1693	0.47608
	0.56351	0.74867	0.25133	474	21097.04	0.18516	0.4334
	0.58679	0.77612	0.22388	473	21141.64	0.18933	0.40964
	0.61208	0.80369	0.19631	472	21186.44	0.19161	0.38541
	0.63965	0.83138	0.16862	471	21231.42	0.19173	0.36004
	0.66983	0.85918	0.14082	470	21276.59	0.18935	0.33251
	0.70298	0.8871	0.1129	469	21321.96	0.18412	0.30121
	0.7396	0.91515	0.08485	468	21367.52	0.17555	0.26335
	0.78023	0.94331	0.05669	467	21413.27	0.16308	0.21336
	0.82559	0.94331	0.05669	467	21413.27	0.11772	0.28448
	0.87655	0.97159	0.02841	466	21459.22	0.09504	0.2076
	0.93421	0.97159	0.02841	466	21459.22	0.03738	0.41521

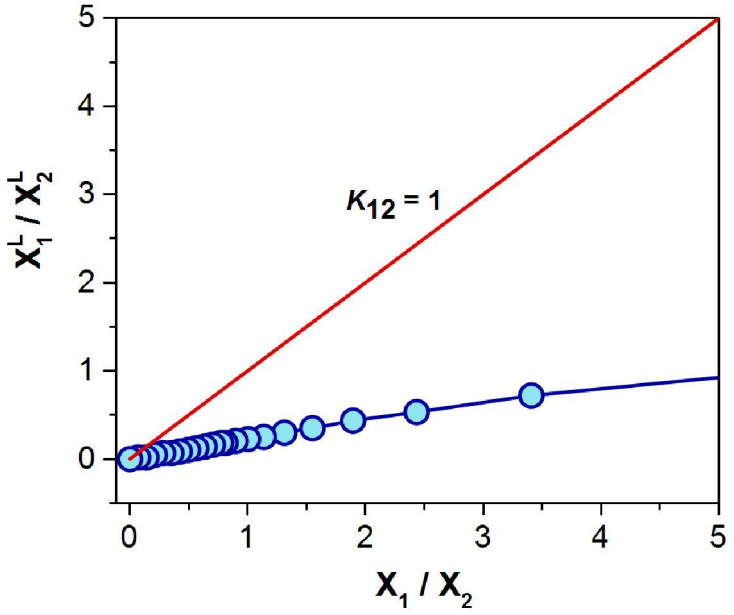

Figure S8. Plot of (X_1^L/X_2^L) versus (X_1/X_2) in the acetonitrile/methanol binary mixture for the solvation of **THA1**. The red line signifies the case when the slope is 1, i.e., $K_{12} = 1$.

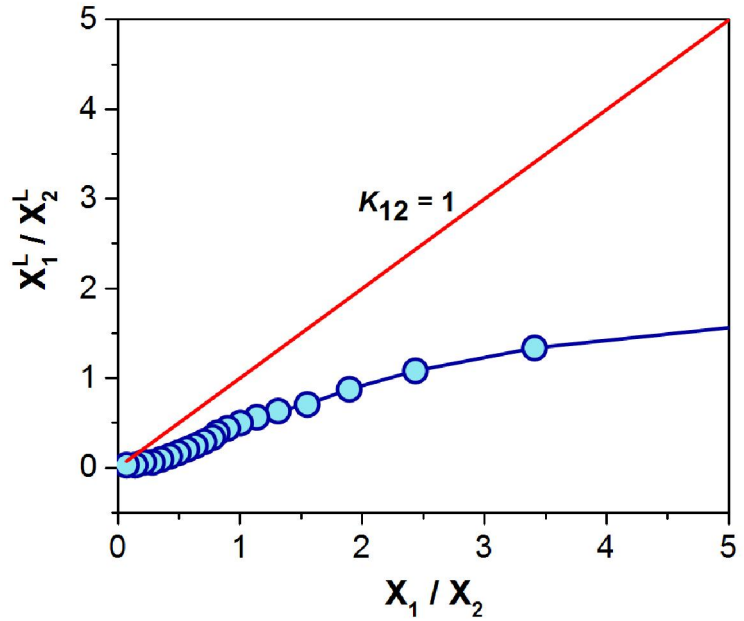

Figure S9. Plot of (X_1^L/X_2^L) versus (X_1/X_2) in the acetonitrile/methanol binary mixture for the solvation of **THA2**. The red line signifies the case when the slope is 1, i.e., $K_{12} = 1$.

Table S3. Kamlet-Taft and Catalán parameters for the solvents used. [a]

Solvent	Kamlet-Taft Parameters			Catalán Parameters			
	α	β	π*	SA	SB	SP	SdP
tetrahydrofuran (THF)	0	0.55	0.58	0	0.48	0.56	0.66
ethyl acetate	0.00	0.45	0.45	0	0.54	0.65	0.60
chloroform	0.20	0.10	0.58	0.05	0.07	0.78	0.61
dichloromethane	0.13	0.10	0.82	0.04	0.17	0.76	0.76
1,2-dichloroethane	0.0	0.0	0.81	0.03	0.13	0.77	0.74
acetone	0.08	0.43	0.71	0	0.47	0.65	0.90
N,N-dimethylacetamide (DMA)	0.00	0.76	0.88	0.03	0.65	0.76	0.99
N,N-dimethylformamide (DMF)	0.00	0.69	0.88	0.03	0.61	0.76	0.98
t-butanol	0.42	0.93	0.41	0.14	0.93	0.63	0.73
dimethyl sulfoxide (DMSO)	0.00	0.76	1.00	0.07	0.65	0.83	1
acetonitrile	0.19	0.40	0.66	0.04	0.29	0.64	0.97
butan-1-ol	0.79	0.88	0.47	0.34	0.81	0.67	0.66
propan-2-ol	0.76	0.84	0.48	0.28	0.83	0.63	0.81
methanol	0.98	0.66	0.60	0.6	0.54	0.61	0.9
ethane-1,2-diol	0.90	0.52	0.92	0.72	0.53	0.78	0.91

[a] The numerical values of the parameters are taken from references 3-7.

Table S4. Experimentally-determined and empirically-calculated E_T(dye) values of **THA1** using Catalán and Kamlet-Taft LSERs in different solvents.

Solvent	E_T(dye) (kcal/mol)		
	Experimental	Calculated from LSER	
		Catalán	Kamlet-Taft
THF	47.41294	47.30201	46.20275
ethyl acetate	47.57072	48.10488	46.20275
chloroform	47.72955	47.73393	48.33359
dichloromethane	46.86885	46.63101	47.14961
1,2-dichloroethane	46.94581	46.67876	46.53698
acetone	45.67093	46.09396	46.54312
DMA	44.25697	44.66105	44.88609
DMF	44.88226	44.75959	45.01838
t-butanol	49.98252	48.62597	48.6947
DMSO	44.25697	44.33599	44.51817
acetonitrile	46.4878	46.30775	47.45734
butan-1-ol	50.15789	50.87148	50.97401
propan-2-ol	49.2931	49.5818	50.82688
methanol	52.65193	52.64554	52.20759
ethane-1,2-diol	52.36264	52.19712	50.97889

Table S5. Experimentally-determined and empirically-calculated E_T(dye) values of **THA2** using Catalán and Kamlet-Taft LSERs in different solvents.

Solvent	E_T(dye) (kcal/mol)		
	Experimental	Calculated from LSER	
		Catalán	Kamlet-Taft
THF	57.06587	56.86821	55.79729
ethyl acetate	56.72619	57.19804	55.99143
chloroform	57.87449	57.45096	57.20398
dichloromethane	57.29459	57.20117	56.75708
1,2-dichloroethane	57.40964	57.16966	56.31194
acetone	56.39053	56.97959	56.21304
DMA	55.51456	56.45886	55.37377
DMF	58.46626	56.50761	55.45641
t-butanol	59.31535	57.76065	57.28667
DMSO	55.51456	56.41779	55.30353
acetonitrile	56.83897	57.41539	56.75922
butan-1-ol	57.29459	59.13504	58.93017
propan-2-ol	59.07025	58.73012	58.84022
methanol	61.48387	61.18531	59.94548
ethane-1,2-diol	61.48387	61.26517	59.57325

Results of DFT Calculations

Table S6. Cartesian coordinates for the optimized structure of **TH1**.

Center Number	Atomic Number	Atomic Type	Coordinates (Angstroms) X	Y	Z
1	6	0	-5.583544	1.027250	-0.273009
2	6	0	-4.217679	0.854477	-0.002079
3	6	0	-3.440175	1.988774	0.271570
4	6	0	-4.015956	3.256325	0.284627
5	6	0	-5.375105	3.415827	0.021959
6	6	0	-6.156119	2.294265	-0.258826
7	1	0	-6.203339	0.170788	-0.512660
8	1	0	-2.384246	1.860926	0.471305
9	1	0	-3.399554	4.122032	0.500265
10	1	0	-5.822076	4.403452	0.030294
11	1	0	-7.212577	2.408075	-0.474834
12	6	0	-3.593218	-0.482324	0.002213
13	6	0	-4.251071	-1.681084	0.006201
14	6	0	-1.822849	-1.806376	0.024016
15	1	0	-5.309457	-1.881648	0.025095
16	7	0	-2.209413	-0.576040	0.017878
17	16	0	-3.120938	-3.006374	0.015452
18	7	0	-0.513599	-2.245840	0.029904
19	1	0	-0.338624	-3.246591	0.048283
20	7	0	0.516356	-1.386419	0.012858
21	6	0	1.706109	-1.870070	0.025437
22	1	0	1.884538	-2.951973	0.050685
23	6	0	2.879173	-1.001567	0.006920
24	6	0	4.159344	-1.578652	0.028963
25	6	0	2.762609	0.400500	-0.032695
26	6	0	5.299565	-0.786854	0.013551
27	1	0	4.261908	-2.657988	0.058693
28	6	0	3.892980	1.199328	-0.048517
29	1	0	1.776138	0.845637	-0.050942
30	6	0	5.150937	0.595394	-0.024910
31	1	0	6.290570	-1.218560	0.030629
32	1	0	3.821091	2.277776	-0.078876
33	7	0	6.355908	1.444447	-0.041052
34	8	0	6.196872	2.659362	-0.074852
35	8	0	7.447609	0.886357	-0.019499

Table S7. Cartesian coordinates for the optimized structure of **THA1**.

Center Number	Atomic Number	Atomic Type	Coordinates (Angstroms) X	Y	Z
1	6	0	-5.173666	1.231980	-0.296868
2	6	0	-3.841164	0.900347	0.000445
3	6	0	-2.956731	1.946042	0.309810
4	6	0	-3.392178	3.268393	0.334181
5	6	0	-4.720084	3.582222	0.047257
6	6	0	-5.608417	2.553003	-0.269704
7	1	0	-5.874416	0.449780	-0.566165
8	1	0	-1.926882	1.698020	0.531768
9	1	0	-2.689059	4.058040	0.578589
10	1	0	-5.058062	4.612828	0.064322
11	1	0	-6.642551	2.781793	-0.506612
12	6	0	-3.362155	-0.495708	-0.004982
13	6	0	-4.164269	-1.608883	-0.011819
14	6	0	-1.720412	-2.027720	0.027027
15	1	0	-5.241749	-1.653012	0.000482
16	7	0	-2.005855	-0.737616	0.020355
17	16	0	-3.208087	-3.053273	0.008119
18	7	0	-0.578470	-2.747449	0.048302
19	7	0	0.630116	-2.194929	0.042360
20	6	0	0.882781	-0.902174	-0.008337
21	1	0	0.099244	-0.152455	-0.051323
22	6	0	2.251721	-0.459765	-0.014305
23	6	0	2.544638	0.927178	-0.079543
24	6	0	3.353368	-1.355509	0.043779
25	6	0	3.842269	1.397149	-0.086788
26	1	0	1.721463	1.632524	-0.126738
27	6	0	4.651741	-0.896095	0.036801
28	1	0	3.140741	-2.415527	0.093327
29	6	0	4.906179	0.485632	-0.028075
30	1	0	4.058598	2.455653	-0.137213
31	1	0	5.488835	-1.579905	0.080533
32	7	0	6.260835	0.967563	-0.035380
33	8	0	7.185844	0.142774	0.016491
34	8	0	6.457297	2.191612	-0.093194

Table S8. Cartesian coordinates for the optimized structure of **TH2**.

Center Number	Atomic Number	Atomic Type	Coordinates (Angstroms) X	Y	Z
1	6	0	-5.222787	0.895472	-0.270747
2	6	0	-3.849867	0.782097	-0.004044
3	6	0	-3.121372	1.949488	0.265460
4	6	0	-3.751304	3.190991	0.279111
5	6	0	-5.116960	3.291328	0.021033
6	6	0	-5.849565	2.136591	-0.255949
7	1	0	-5.805771	0.012622	-0.507024
8	1	0	-2.060261	1.867397	0.461694
9	1	0	-3.172162	4.082833	0.491640
10	1	0	-5.606316	4.258666	0.029858
11	1	0	-6.910719	2.204277	-0.468396
12	6	0	-3.167417	-0.526172	0.000944
13	6	0	-3.772122	-1.752305	0.004925
14	6	0	-1.339602	-1.770453	0.026193
15	1	0	-4.820668	-1.999157	0.022548
16	7	0	-1.780722	-0.558379	0.018487
17	16	0	-2.584339	-3.026831	0.016706
18	7	0	-0.013326	-2.151785	0.034756
19	1	0	0.206108	-3.143513	0.055323
20	7	0	0.979058	-1.246268	0.014221
21	6	0	2.188077	-1.677537	0.028537
22	1	0	2.413113	-2.750870	0.058114
23	6	0	3.324569	-0.760565	0.006028
24	6	0	4.627647	-1.280793	0.028924
25	6	0	3.150791	0.634579	-0.038832
26	6	0	5.731977	-0.440333	0.008783
27	1	0	4.776594	-2.354820	0.062976
28	6	0	4.246961	1.478370	-0.059291
29	1	0	2.146378	1.038113	-0.057420
30	6	0	5.549671	0.948372	-0.035586
31	1	0	6.734289	-0.849852	0.026804
32	1	0	4.109438	2.552139	-0.093941
33	6	0	6.681652	1.821081	-0.056635
34	7	0	7.597462	2.526461	-0.073548

Table S9. Cartesian coordinates for the optimized structure of **THA2**.

Center Number	Atomic Number	Atomic Type	Coordinates (Angstroms) X	Y	Z
1	6	0	-4.820020	1.133369	-0.244855
2	6	0	-3.466138	0.846231	-0.000081
3	6	0	-2.602553	1.924723	0.252019
4	6	0	-3.076951	3.233844	0.270703
5	6	0	-4.424659	3.502949	0.035311
6	6	0	-5.293316	2.441030	-0.224394
7	1	0	-5.508469	0.325833	-0.466644
8	1	0	-1.557398	1.710690	0.433855
9	1	0	-2.388432	4.048710	0.470491
10	1	0	-4.793089	4.523214	0.047980
11	1	0	-6.343535	2.633815	-0.419375
12	6	0	-2.943369	-0.533887	-0.002918
13	6	0	-3.710222	-1.670843	-0.004390
14	6	0	-1.248686	-2.011474	0.023823
15	1	0	-4.785725	-1.749547	0.009392
16	7	0	-1.578932	-0.730251	0.015822
17	16	0	-2.708151	-3.086309	0.013331
18	7	0	-0.087762	-2.690655	0.040808
19	7	0	1.104776	-2.089282	0.034720
20	6	0	1.310483	-0.793467	-0.009048
21	1	0	0.503386	-0.068374	-0.045845
22	6	0	2.670533	-0.301276	-0.015674
23	6	0	2.918657	1.090756	-0.074550
24	6	0	3.798894	-1.157974	0.035319
25	6	0	4.203915	1.602245	-0.082083
26	1	0	2.073854	1.770738	-0.116360
27	6	0	5.083302	-0.654364	0.027927
28	1	0	3.620799	-2.224896	0.079877
29	6	0	5.314037	0.738025	-0.030659
30	1	0	4.365417	2.673537	-0.127845
31	1	0	5.932206	-1.328299	0.067477
32	6	0	6.638338	1.256567	-0.037429
33	7	0	7.718767	1.679730	-0.042840

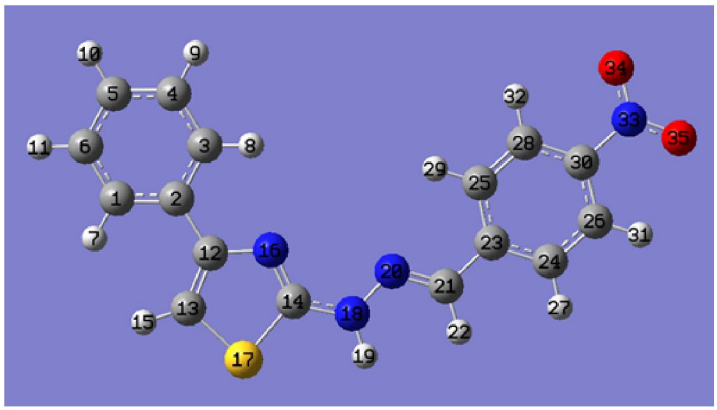

TH1

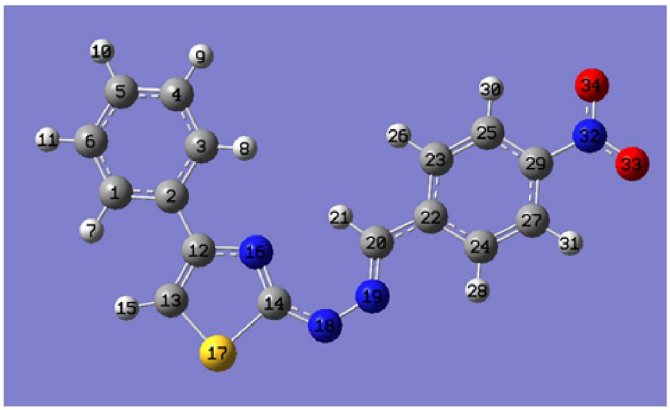

THA1

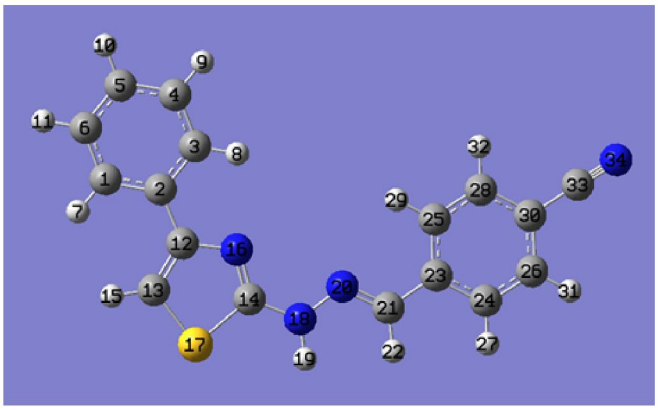

TH2

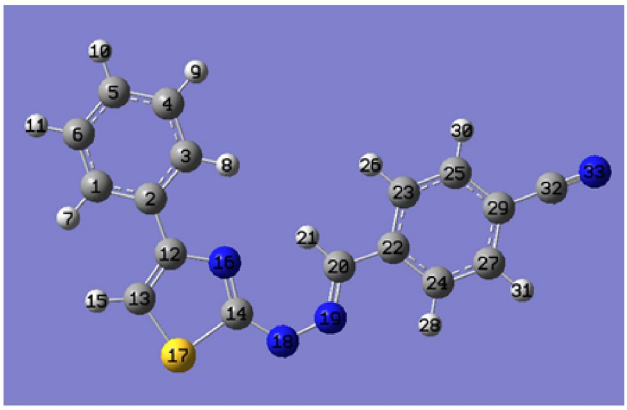

THA2

Figure S10. Structures of the **TH**s and **THA**s optimized by using DFT/B3LYP/6-311++G(d,p) level of theory.

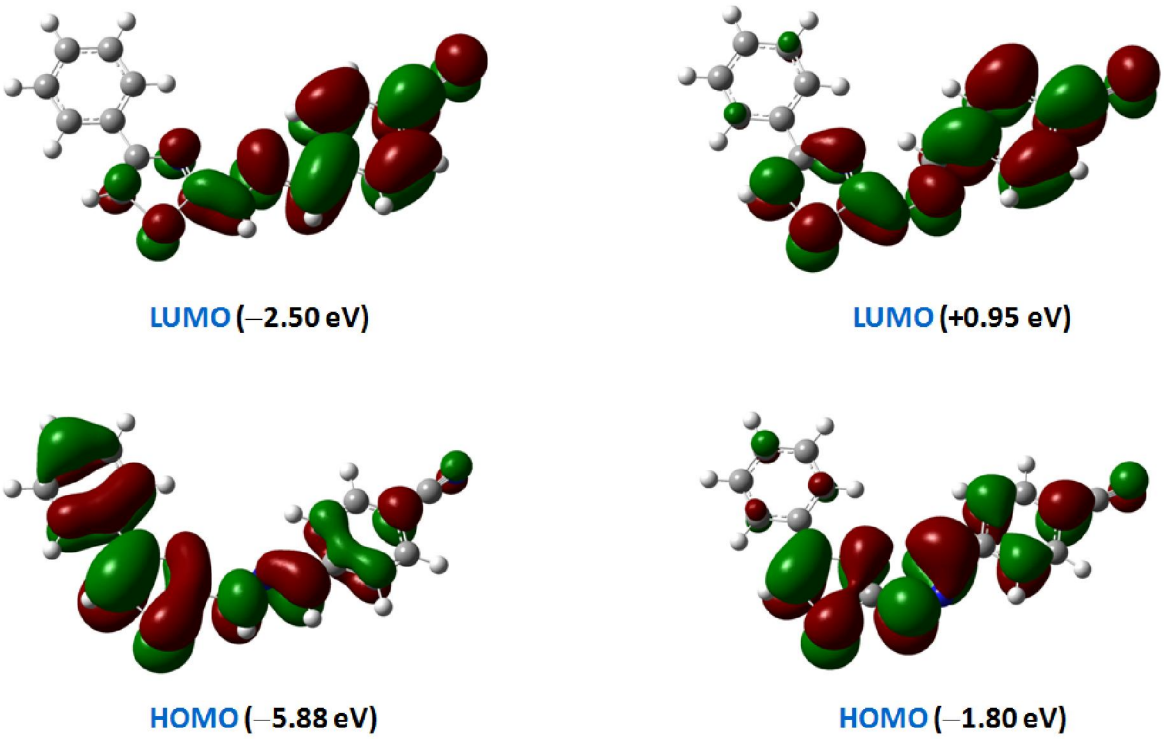

Figure S11. Contour plots for the frontier molecular orbitals (HOMO and LUMO) of **TH2** (left) and **THA2** (right); the structures were optimized by using DFT/B3LYP/6-311++G(d,p) level of theory. Note that the energies of the MOs are shown in the parentheses.

Results of NBO Analyses

Table S10. Second order perturbation theory analysis of Fock matrix in NBO basis for the hetero atoms containing lone pairs in **TH1**.

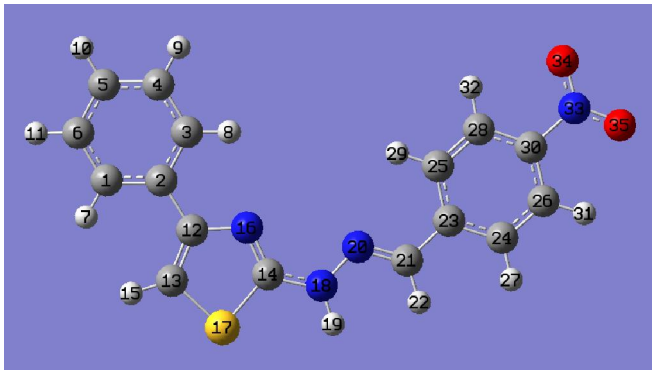

Donor NBO (i)	Acceptor NBO (j)	E^2 (kcal/mol)	E(j)-E(i) (a.u.)	F(i,j) (a.u.)
75. LP (1) N16	/567. BD*(1) C12 - C13	2.96	0.77	0.043
76. LP (1) S17	/567. BD*(1) C12 - C13	7.94	0.91	0.076
77. LP (2) S17	/567. BD*(1) C12 - C13	0.55	0.62	0.020
78. LP (1) N18	/572. BD*(1) C14 - N16	8.20	0.84	0.075
78. LP (1) N18	/573. BD*(2) C14 - N16	3.53	0.33	0.034
78. LP (1) N18	/574. BD*(1) C14 - S17	0.82	0.84	0.024
78. LP (1) N18	/578. BD*(1) N20 - C21	3.53	0.96	0.053
78. LP (1) N18	/579. BD*(2) N20 - C21	3.61	0.37	0.033
79. LP (1) N20	/581. BD*(1) C21 - C23	16.96	0.60	0.092
80. LP (1) O34	/595. BD*(1) C30 - N33	4.29	1.07	0.062
80. LP (1) O34	/597. BD*(1) N33 - O35	2.31	1.27	0.049
81. LP (2) O34	/590. BD*(1) C26 - C30	0.70	0.84	0.022
81. LP (2) O34	/595. BD*(1) C30 - N33	14.50	0.57	0.081
81. LP (2) O34	/597. BD*(1) N33 - O35	19.72	0.77	0.112
82. LP (3) O34	/598. BD*(2) N33 - O35	171.84	0.15	0.146
83. LP (1) O35	/595. BD*(1) C30 - N33	4.29	1.06	0.062
83. LP (1) O35	/596. BD*(1) N33 - O34	2.30	1.27	0.049
84. LP (2) O35	/593. BD*(1) C28 - C30	0.70	0.84	0.022
84. LP (2) O35	/595. BD*(1) C30 - N33	14.48	0.57	0.081
84. LP (2) O35	/596. BD*(1) N33 - O34	19.74	0.77	0.112

Table S11. Second order perturbation theory analysis of Fock matrix in NBO basis for the hetero atoms containing lone pairs in **THA1**.

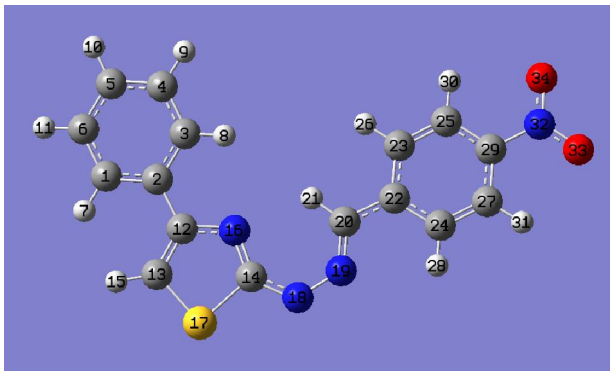

Donor NBO (i)	Acceptor NBO (j)	E^2 (kcal/mol)	E(j)-E(i) (a.u.)	F(i,j) (a.u.)
75. LP (1) N16	/561. BD*(1) C12 - C13	3.10	0.75	0.043
75. LP (1) N16	/568. BD*(1) C14 - S17	5.99	0.86	0.064
75. LP (1) N16	/569. BD*(1) C14 - N18	1.23	0.73	0.027
76. LP (1) S17	/561. BD*(1) C12 - C13	8.43	0.90	0.078
76. LP (1) S17	/566. BD*(1) C14 - N16	6.52	1.03	0.073
77. LP (1) N18	/566. BD*(1) C14 - N16	8.46	0.92	0.080
77. LP (1) N18	/571. BD*(1) N19 - C20	8.90	1.03	0.087
77. LP (1) N18	/572. BD*(2) N19 - C20	5.13	0.43	0.043
78. LP (2) N18	/566. BD*(1) C14 - N16	0.81	0.69	0.024
78. LP (2) N18	/567. BD*(2) C14 - N16	45.43	0.18	0.082
78. LP (2) N18	/568. BD*(1) C14 - S17	0.95	0.68	0.026
78. LP (2) N18	/572. BD*(2) N19 - C20	12.04	0.20	0.048
79. LP (1) N19	/569. BD*(1) C14 - N18	1.28	0.56	0.025
79. LP (1) N19	/572. BD*(2) N19 - C20	1.97	0.22	0.019
79. LP (1) N19	/574. BD*(1) C20 - C22	16.13	0.59	0.092
80. LP (1) O33	/588. BD*(1) C29 - N32	4.28	1.07	0.062
80. LP (1) O33	/591. BD*(1) N32 - O34	2.36	1.27	0.049
81. LP (2) O33	/580. BD*(1) C24 - C27	0.51	0.87	0.019
81. LP (2) O33	/583. BD*(1) C25 - C29	0.70	0.84	0.022
81. LP (2) O33	/588. BD*(1) C29 - N32	14.08	0.58	0.081
81. LP (2) O33	/591. BD*(1) N32 - O34	19.92	0.78	0.112
82. LP (1) O34	/588. BD*(1) C29 - N32	4.29	1.07	0.062
82. LP (1) O34	/589. BD*(1) N32 - O33	2.35	1.27	0.049
83. LP (2) O34	/578. BD*(1) C23 - C25	0.51	0.86	0.019
83. LP (2) O34	/586. BD*(1) C27 - C29	0.70	0.85	0.022
83. LP (2) O34	/588. BD*(1) C29 - N32	14.04	0.58	0.080
83. LP (2) O34	/589. BD*(1) N32 - O33	19.91	0.78	0.113
84. LP (3) O34	/584. BD*(2) C25 - C29	0.55	0.29	0.011
84. LP (3) O34	/590. BD*(2) N32 - O33	155.35	0.15	0.145

Table S12. Second order perturbation theory analysis of Fock matrix in NBO basis for the hetero atoms containing lone pairs in **TH2**.

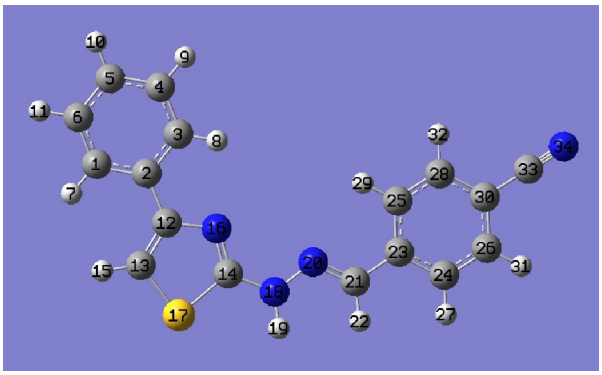

Donor NBO (i)	Acceptor NBO (j)	E^2 (kcal/mol)	E(j)-E(i) (a.u.)	F(i,j) (a.u.)
74. LP (1) N16	/546. BD*(1) C12 - C13	2.96	0.77	0.043
74. LP (1) N16	/553. BD*(1) C14 - S17	5.65	0.87	0.063
74. LP (1) N16	/554. BD*(1) C14 - N18	1.50	0.69	0.029
75. LP (1) S17	/546. BD*(1) C12 - C13	7.90	0.91	0.076
75. LP (1) S17	/551. BD*(1) C14 - N16	6.54	1.01	0.073
76. LP (1) N18	/551. BD*(1) C14 - N16	8.22	0.84	0.075
76. LP (1) N18	/552. BD*(2) C14 - N16	3.54	0.33	0.034
76. LP (1) N18	/553. BD*(1) C14 - S17	0.81	0.84	0.024
76. LP (1) N18	/557. BD*(1) N20 - C21	3.53	0.96	0.053
76. LP (1) N18	/558. BD*(2) N20 - C21	3.47	0.38	0.032
77. LP (1) N20	/560. BD*(1) C21 - C23	16.91	0.60	0.092
80. LP (1) N34	/573. BD*(1) C30 - C33	10.97	0.87	0.087

Table S13. Second order perturbation theory analysis of Fock matrix in NBO basis for the hetero atoms containing lone pairs in **THA2**.

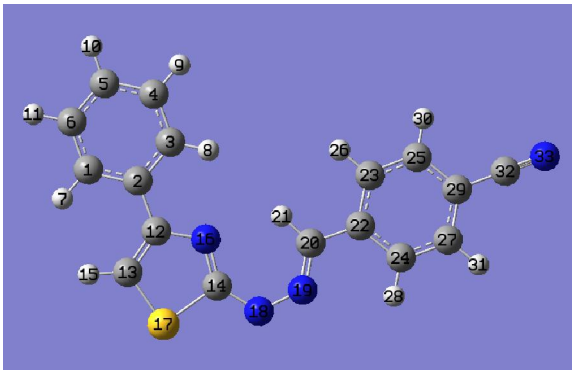

Donor NBO (i)	Acceptor NBO (j)	E^2 (kcal/mol)	E(j)-E(i) (a.u.)	F(i,j) (a.u.)
74. LP (1) N16	/539. BD*(1) C12 - C13	3.11	0.74	0.043
74. LP (1) N16	/546. BD*(1) C14 - S17	6.04	0.86	0.065
74. LP (1) N16	/547. BD*(1) C14 - N18	1.21	0.73	0.027
75. LP (1) S17	/539. BD*(1) C12 - C13	8.53	0.90	0.079
75. LP (1) S17	/544. BD*(1) C14 - N16	6.50	1.03	0.073
76. LP (1) N18	/544. BD*(1) C14 - N16	8.58	0.91	0.080
76. LP (1) N18	/549. BD*(1) N19 - C20	8.95	1.02	0.087
76. LP (1) N18	/550. BD*(2) N19 - C20	5.95	0.43	0.046
77. LP (2) N18	/544. BD*(1) C14 - N16	0.77	0.69	0.023
77. LP (2) N18	/545. BD*(2) C14 - N16	45.22	0.18	0.083
77. LP (2) N18	/546. BD*(1) C14 - S17	0.96	0.68	0.025
77. LP (2) N18	/550. BD*(2) N19 - C20	10.65	0.20	0.044
78. LP (1) N19	/547. BD*(1) C14 - N18	0.98	0.56	0.022
78. LP (1) N19	/550. BD*(2) N19 - C20	0.91	0.22	0.013
78. LP (1) N19	/552. BD*(1) C20 - C22	17.51	0.58	0.094
79. LP (1) N33	/566. BD*(1) C29 - C32	10.53	0.88	0.086

References

1. R. I. Stock, L. G. Nandi, C. R. Nicoleti, A. D. S. Schramm, S. L. Meller, R. S. Heying, D. F. Coimbra, K. F. Andriani, G. F. Caramori, A. J. Bortoluzzi and V. G. Machado, *J. Org. Chem.*, 2015, **80**, 7971−7983.
2. C. T. Martins, M. S. Lima, E. L. Bastos, and O. A. El Seoud, *Eur. J. Org. Chem.*, 2008, 1165–1180.
3. J. Catalán, *J. Phys. Chem. B*, 2009, **113**, 5951–5960.
4. N. Friebe, K. Schreiter, J. Kübel, B. Dietzek, N. Moszner, P. Burtscher, A. Oehlkea and S. Spange, *New J. Chem.*, 2015, **39**, 5171–5179.
5. L. G. Nandi, F. Facin, V. G. Marini, L. M. Zimmermann, L. A. Giusti, R. da Silva, G. F. Caramori and V. G. Machado, *J. Org. Chem.*, 2012, **77**, 10668−10679.
6. R. I. Stock, L. G. Nandi, C. R. Nicoleti, A. D. S. Schramm, S. L. Meller, R. S. Heying, D. F. Coimbra, K. F. Andriani, G. F. Caramori, A. J. Bortoluzzi and V. G. Machado, *J. Org. Chem.*, 2015, **80**, 7971−7983.
7. R. I. Stock, A. D. S. Schramm, M. C. Rezende and V. G. Machado, *Phys. Chem. Chem. Phys.*, 2016, **18**, 20266–20269.